Atmospheric neutrino oscillation analysis with sub-leading effects in Super-Kamiokande

Chizue ISHIHARA* **for Super-Kamiokande Collaboration**

ICRR, Univ. of Tokyo

***Abstract*. The atmospheric neutrino data have been well measured 2-3 oscillation parameters. If 1-2 parameters are considered in atmospheric neutrino oscillation analysis, the oscillation of low energy atmospheric ν_e could be observed. The ν_e flux change depends on the octant of θ_{23} ($\theta_{23} > \pi/4$ or $< \pi/4$). This paper presents a search for deviations of sin$^2\theta_{23}$ from 0.5 in the atmospheric neutrino data of Super-Kamiokande I, II and III by taking account the sub-leading oscillation driven by 1-2 parameters. There is no significant discrepancy of θ_{23} from $\pi/4$. sin$^2\theta_{23}$ is determined $0.44 \leq$ sin$^2\theta_{23} \leq 0.56$ in 1-σ C.L., which is stronger constraint on sin$^2\theta_{23}$ than a case without 1-2 parameters.**

***Keywords*: atmospheric neutrino Super-Kamiokande**

I. INTRODUCTION

Neutrino oscillation is proposed by Maki, Nakagawa and Sakata as a consequence of the finite masses of neutrino [1]. Three flavor eigenstates can be written as the superpositions of the mass eigenstates as

$$|\nu_\alpha\rangle = \sum_i^3 U_{\alpha,i}|\nu_i\rangle,$$

$U_{\alpha,i}$ is a mixing matrix known as MNS matrix which can be written as three rotation matrices using the mixing angles. Each mixing angle parameterizes the rotation between pairs of mass states inside of the three-dimensional oscillation space. Neutrino oscillation parameters are represented by six parameters: two mass squared differences (Δm$^2_{23}$, Δm$^2_{12}$), three mixing angles (θ_{12} , θ_{23} , θ_{13}) and CP-violating phase δ.

Lots of neutrino experiments have been measuring the neutrino oscillation precisely, then the oscillation parameters have been well understood. Atmospheric neutrino data in Super-Kamiokande(SK) experiment have been established 2-flavor ($\nu_\mu \leftrightarrow \nu_\tau$) neutrino mixing phenomenon, and well measured Δm$^2_{23}$ and the mixing angle (2-3 parameters) [4][5], known as maximal mixing sin$^2 2\theta_{23} \simeq 1.0$ ($\theta_{23} \simeq \pi/4$). If sin$^2 2\theta_{23}$ is not maximal, $\theta_{23} \neq \pi/4$, it makes two solutions of θ_{23} which can be cause of degeneracy solutions on future θ_{13} and CP-δ measurement experiments [6].

On the other hand, the solar neutrino parameters Δm$^2_{12}$ and sin$^2\theta_{12}$ have been measured accurately by solar neutrino data [7][8] and KamLAND reactor neutrino data [9].

The third mixing angle parameter θ_{13} has been thought to be very small, which is probed by Chooz experiment placing a limit on it at sin$^2\theta_{13} < 0.04$ for $\Delta m^2 \sim 2.0 \times 10^{-3}$ eV^2 at 90% confidence[3]. And sin$^2\theta_{13}$ is consistent with zero value in atmospheric neutrino data.

For $\theta_{13} \sim 0$, if solar neutrino parameters (1-2 parameters) are taken into account, the atmospheric ν_e oscillation is expected to appear in low energy region ($E_\nu <$ 1GeV). And, this phenomenon can provide us the information of the octant of θ_{23} ($\theta_{23} > \pi/4$ or $\theta_{23} < \pi/4$) by using change of e-like sample.

In this paper, we describe a result of the θ_{23} determination in Super-Kamiokande atmospheric neutrino data using sub-dominant oscillations driven by the solar neutrino parameters.

II. SUB-LEADING OSCILLATION EFFECTS DRIVEN BY 1-2 PARAMETERS

In the case of $\theta_{13} \sim 0$ the neutrino oscillation probabilities in constant density matter may be written [2]:

$$\begin{aligned} P(\nu_e \leftrightarrow \nu_e) &= 1 - P_{ex} \\ P(\nu_e \leftrightarrow \nu_\mu) &= \cos^2\theta_{23} P_{ex} \end{aligned}$$

where P_{ex} is the transition probability from $\nu_e \leftrightarrow \nu_x$ (x = μ or τ) in matter driven by Δm$^2_{12}$ and θ_{12} . Using these equations the modified atmospheric ν_e fluxes at SK become

$$\begin{aligned} \Phi_e &= \Phi_e^0 P(\nu_e \leftrightarrow \nu_e) + \Phi_\mu^0 P(\nu_\mu \leftrightarrow \nu_e) \\ &= \Phi_e^0 \left[1 + P_{ex}\left(r\cos^2\theta_{23} - 1\right)\right] \end{aligned} \quad (1)$$

where Φ_μ^0 and Φ_e^0 are the neutrino fluxes in the absence of oscillations and r is their ratio Φ_μ^0/Φ_e^0.

Figure 1 shows the disappearance probability, P_{ex}, as a function of energy and zenith angle , Θ_ν, for neutrinos traversing the Earth assuming $\Delta m^2_{12} = 7.7 \times 10^{-5}$ eV^2 and sin$^2\theta_{12}$ = 0.30. However, the overall effect of P_{ex} on the electron neutrino flux at the detector is moderated by the factor $r\cos^2\theta_{23} - 1$ as seen in equation (1). Since the atmospheric neutrino flux ratio is $r \sim 2$ at low energies, there is no change in the ν_e flux if $\cos^2\theta_{23} = 0.5$ ($\theta_{23} = \pi/4$). On the other hand, if $\cos^2\theta_{23}$ is greater (less) than 0.5 ($\theta_{23} < (>)\pi/4$) there is an expected enhancement (reduction) of the flux. Therefore it may be possible to determine the octant of θ_{23} by searching for changes in the flux of the low energy electron-like samples at SK.

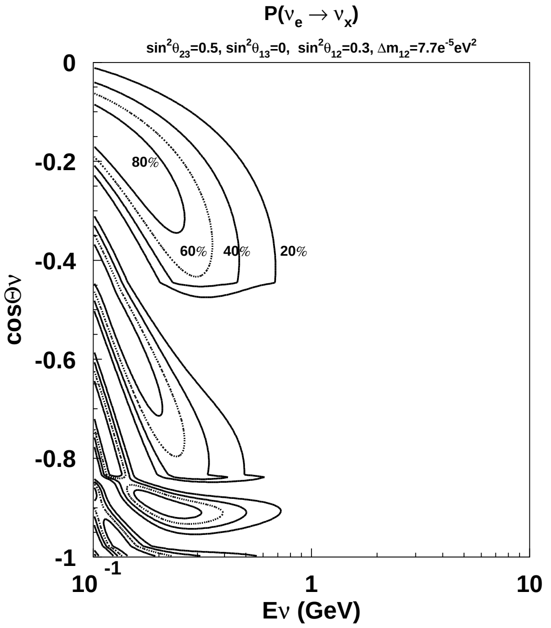

Fig. 1. The calculated ν_e transition probability P_{ex} for atmospheric neutrinos with an energy E_ν and direction $\cos\Theta_\nu$. The 1-2 oscillation parameters are taken to be $\Delta m^2_{12} = 7.7 \times 10^{-5} eV^2$ and $\sin^2\theta_{12} = 0.30$. Matter effects within the Earth are taken into account.

III. Data sample

Super-Kamiokande is a cylindrical 50 kton water Cherenkov detector situated at a depth of 2700 meters water equivalent. The detector volume is optically separated into an inner volume (ID) and an outer veto region (OD). During each SK phase, SK-I, SK-II and SK-III period, livetime is 1489 days , 799 days and 518 days, respectively.

We observe the fully contained (FC), partially contained (PC) and upward-going muons (UPμ) events, and they are compared with expectation by 500 years Monte Carlo simulation for each SK phase.

Fully contained events are further divided into sub-GeV and multi-GeV subsamples based on the events visible energy, E_{vis} . Events with $E_{\text{vis}} < 1.33$ GeV are categorized as sub-GeV sample. The number of reconstructed Cherenkov rings in an event is also used to separate these samples into single- and multi-ring subsamples. Single-ring events are classified into muon-like (μ-like) and electron-like (e-like) samples by the ring pattern. For multi-ring samples, the most energetic ring is used to identify the particle type. Partially contained events are classified as “OD stopping” or “OD through-going” based on their energy deposition in the OD [4]. Similarly UPμevents that traverse the detector are separated into “showering” and “non-showering” based on the method in ref. [10] while those that enter and stop within the ID detector are classified as “stopping.”

To increase the purity of the interaction mode, FC sub-GeV single-ring events are separated into subsamples based on their number of decay electrons and how π^0-like they are. The FC sub-GeV single-ring e-like sample contains background events which are mainly neutral-current (NC) π^0 events where one of the two γ rays from the π^0 decay has been missed by the event reconstruction. The electromagnetic shower from the γ gives a light pattern similar to that of an electron and results in an electron-like classification. To reduce this type of background a specialized π^0 fitter is used. After separating the π^0-like sample, the remaining e-like events are divided into two categories, 0-DKe which has no decay electrons and 1-DKe which has one or more decay electrons. For the FC sub-GeV single-ring μ-like sample, there are three categories using the number of decay electrons: 0-DKμ, 1-DKμ and 2-DKμ, corresponding to no decay electron, 1 decay electron and 2 or more decay electrons respectively. Since these sub-samples have a high fraction of CCQE events they are useful tools to search for changes in the low energy ν_e induced by the solar oscillation parameters therefore improving the analysis' sensitivity to $\theta_{23} \neq \pi/4$.

IV. Oscillation analysis

The oscillation analyses have been performed using the above data samples. Since the physical detector configuration differs among SK-I, SK-II and SK-III separate 500 years equivalent MC data sets for each run period are used. The data are compared against the MC expectation using a “pulled” χ^2 method based on a Poisson probability distribution:

$$\begin{aligned}\chi^2 &= 2\sum_n \Bigg(E_n(1+\sum_i f_n^i \epsilon_i) - \mathcal{O}_n \\ &+ \mathcal{O}_n \ln \frac{\mathcal{O}_n}{E_n(1+\sum_i f_n^i \epsilon_i)} \Bigg) \\ &+ \sum_i \left(\frac{\epsilon_i}{\sigma_i}\right)^2 + \Delta\chi^2_{solar},\end{aligned}$$

where n indexes the data bins, E_n is the MC expectation and $\mathcal{O}_n$ is the number of observed events in the n^{th} bin. Systematic errors are incorporated into the fit via the systematic error parameter ϵ_i, where i is the systematic error index, f_n^i is the fractional change in the MC expectation in bin n for a 1-sigma change in the i^{th} systematic error. The 1-sigma value of a systematic error is labeled as σ_i.

The decay electron samples are divided into 5 momentum. Furthermore the 0-DKe, 0-DKμ and 1-DKμ samples are divided into 10 zenith angle bins. Other FC events are divided into 14 momentum bins, PC events into 6 bins and UPμevents into 5. All of these samples are further divided into 10 evenly spaced zenith angle bins. FC and PC events range from $-1 \leq \cos\Theta \leq 1$ and UPμevents are binned from $-1 \leq \cos\Theta \leq 0$.

The systematic errors are separated into two categories, common among SK phases and not. Errors that are classified as common are related to uncertainties in the atmospheric neutrino flux and neutrino interaction. Systematic errors that are independent among SK phases represent uncertainties related to the detector performance in each era. All systematics are considered to be uncorrelated.

SK-II and SK-III data bins have lower statistics so they are combined into SK-I, while preserving the effect of separated systematic errors for each SK phase. In this method, the fitting to find the systematic error parameter ϵ_i is performed over all bins in SK-I, II and III simultaneously, but the pulled expectation $E_n(1+\sum f^i\epsilon_i)$ of SK-II and SK-III bins are merged into same categorized bins of SK-I. Then larger numerical values help buffer χ^2 value against fluctuations in a given bin.

In this analysis, two scenarios are performed to the data to extract a constraint on $\sin^2\theta_{23}$. The first (solar-off) is done over the two dimensional space of Δm^2_{23} and $\sin^2\theta_{23}$ and is compared to a second (solar-on) fit, expanded to four dimensions including the solar oscillation parameters $(\Delta m^2_{12}, \sin^2\theta_{12})$. The grid of points chosen over these terms is based on a combined fit of the solar neutrino experiment and KamLAND data[11]. To constrain the fit over the solar parameters the $\Delta\chi^2_{solar}$ value from this combined analysis is then added to that of the fit at each of these grid points.

Figure 2 shows the $\Delta\chi^2$ distributions with and without the solar parameters as function of $\sin^2\theta_{23}$, where $\Delta m^2_{12}, \Delta m^2_{23}$ and $\sin^2\theta_{12}$ are chosen so that χ^2 is minimized. The best-fit point with (without) the solar parameters is located at $\sin^2\theta_{23} = 0.51(0.50)$ with a minimum χ^2 / d.o.f. value of 471.4 / 416 (470.4 / 418) and the atmospheric mass splitting is fit to $\Delta m^2_{23} = 2.1\times10^{-3}$ eV^2. In the solar-on fit the solar oscillation parameters are best fit to $\Delta m^2_{12} = 7.59\times10^{-5}$ eV^2 and $\sin^2\theta_{12} = 0.30$.

No significant deviation of $\sin^2\theta_{23}$ from $\pi/4$ is seen with the addition of solar terms to the analysis but they do give rise to the asymmetric shape seen in the χ^2 distribution. The stringent constraint on $\sin^2\theta_{23}$ has been observed with the solar terms. The 1-σ arrowed region ($\Delta\chi^2$=1.0) is $0.44 < \sin^2\theta_{23} < 0.56$.

V. Conclusion

The search for deviations from maximal atmospheric mixing finds no evidence for a preferred octant for θ_{23} . However, the mixing angle is constrained at 1-sigma C.L. to $0.44 < \sin^2\theta_{23} < 0.56$.

Acknowledgments

This work was supported in part by Global COE Program (Global Center of Excellence for Physical Sciences Frontier), MEXT, Japan.

References

[1] Z. Maki, M. Nakagawa, and S. Sakata, Prog. Theo. Phys. 28(1962)870
[2] O.L.G Peres and A. Yu. Smirnov, Phys. Lett.b456(1999)204
[3] M. Apollonio et al., Phys. Lett.B 466(1999)
[4] Y. Ashie et al. (Super-Kamiokande collaboration), Phys. Rev. Lett.93(2004)101801, hep-ex/0404034
[5] Y. Ashie et al. (Super-Kamiokande collaboration), Phys. Rev. D71(2005)112005, hep-ex/0501064

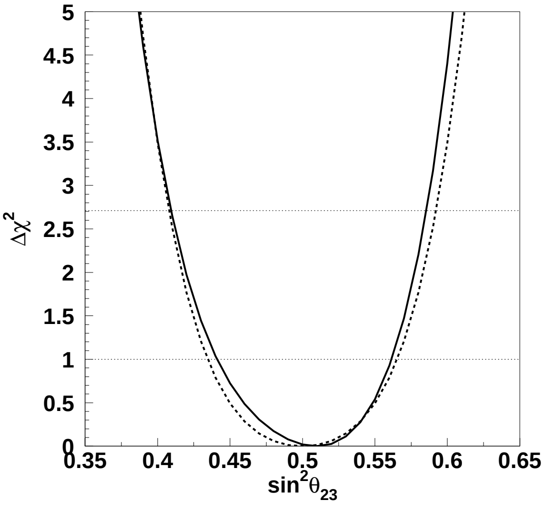

Fig. 2. χ^2-χ^2_{min} distribution as a function of $\sin^2\theta_{23}$ for oscillations without the 1-2 parameters (dotted line) and with the 1-2 parameters (solid line). For each $\sin^2\theta_{23}$ point, Δm^2_{23} is chosen so that χ^2 is minimized.

[6] V. Barger, D. Marfatia and K. Wisnant, Phys. Rev.D65(2002)073023
[7] B. Aharmim et al. (SNO collaboration), Phys. Rev. Lett.101(2008)111301, hep-ph/0806.0989
[8] J. Hosaka et al. (Super-Kamiokande collaboration), Phys. Rev. D73(2006)112001
[9] S. Abe et al.(The KamLAND collaboration),hep-ph/0801.4589
[10] S. Desai, et al, Astropart. Phys.19(2008)42
[11] G. L. Fogli et al, 2008, hep-ph/0808.2016